Available online at www.sciencedirect.com

SciVerse ScienceDirect

Scripta Materialia 65 (2011) 1018–1021

Scripta MATERIALIA

www.elsevier.com/locate/scriptamat

Preparation of zirconium diboride ceramics by reactive spark plasma sintering of zirconium hydride–boron powders

Shuqi Guo,[a,*] Toshiyuki Nishimura[b] and Yutaka Kagawa[a,c]

[a]*Hybrid Materials Unit, National Institute for Materials Science, 1-2-1 Sengen, Tsukuba, Ibaraki 305-0047, Japan*
[b]*Sialon unit, National Institute for Materials Science, 1-1 Namiki, Tsukuba, Ibaraki 305-0044, Japan*
[c]*Research Center for Advanced Science and Technology, The University of Tokyo, 4-6-1 Komaba, Meguro-ku, Tokyo 153-8505, Japan*

Received 9 August 2011; revised 1 September 2011; accepted 3 September 2011
Available online 10 September 2011

Monolithic ZrB_2 ceramics were prepared by reactive spark plasma sintering of a ZrH_2–B mixture at 1650–1800 °C. The microstructure of the resulting ZrB_2 ceramics were characterized by X-ray diffractometry and scanning electron microscopy. The ZrH_2–B mixture converted completely into ZrB_2 without trace quantities of residual ZrH_2 and B. Highly dense ZrB_2 was obtained at 1750 °C or above. The elastic moduli, flexural strength, thermal and electrical conductivities were comparable with those of ZrB_2 ceramics obtained by sintering conventional ZrB_2 powders.

Keywords: Zirconium diboride; Zirconium hydride; Boron; Reactive spark plasma sintering

Zirconium diboride (ZrB_2) has an extremely high melting point (>3000 °C), high thermal and electrical conductivities, chemical inertness against molten metals, and good thermal shock resistance [1,2]. Thus, ZrB_2 ceramics have become an important class of materials for structural applications at 1800 °C or above. However, the densification of ZrB_2 powder generally requires very high temperatures (>2100 °C) and external pressure because of the material's strong covalent bonding and low self-diffusivity [2–4]. To improve sinterability, nitrides (AlN, Si_3N_4, ZrN) [5–7], carbides (SiC, B_4C) [8,9], silicides ($MoSi_2$, $ZrSi_2$) [10,11], and metals (Ni, Co) [12] are added to ZrB_2, producing an intergranular liquid phase that aids its densification. These additives significantly improve the sinterability of ZrB_2, but drastically reduce its high-temperature strength [13,14]. An alternative potential approach to obtaining ZrB_2 ceramics that offer good high-temperature mechanical performance is to sinter reactive precursor reactants.

Recently, SiC-containing ZrB_2 ceramics have been developed at 1800 °C or above, by the reaction of Zr, B_4C and Si precursor powders [15,16]. More recently, Brochu et al. [17] prepared singe-phase ZrB_2 at temperatures ranging from 1600 to 2000 °C by the reaction of Zr and B powders. Although the mixture of Zr and B completely converted into ZrB_2, only a theoretical density of 72% was obtained for the converted ZrB_2. Therefore, it is required in order to develop highly dense ZrB_2 ceramics sintered at lower temperatures to explore new precursor reactants as well as densification methods. In the present study, monolithic ZrB_2 ceramics were prepared in situ by reactive spark plasma sintering (SPS) of ZrH_2 and B powders at various temperatures 1650–1800 °C. The microstructure, densification behavior, elastic moduli, flexural strength, thermal and electrical conductivities are discussed.

The starting powders used in this study were zirconium(II) hydride (ZrH_2) powder (325 mesh, purity 99%, Sigma–Aldrich, Inc., Louis, MO, USA) and amorphous boron (B) powder ($d_{50} = 0.8$ μm, purity 95.9%, H.C. Starck GmbH, Germany). Starting powders were weighed in stoichiometric proportions according to following reaction:

$$ZrH_2 + 2B \rightarrow ZrB_2 + H_2 \quad (1)$$

The B and ZrH_2 powders were wet-ball milled for 24 h in SiC media using alcohol as a solvent, and the resulting slurry was then dried. Before sintering, the dried powders were sieved through a metallic sieve with 60-mesh screen size. Figure 1 shows scanning electron microscopy images of as-received ZrH_2, B and the milled powder mixture. The morphologies of both the as-received powders were similar, showing a bimodal particle size distribution. After the milling (Fig. 1c),

* Corresponding author. Tel.: +81 (0)29 859 2223; fax: +81 (0)29 859 2401; e-mail: GUO.Shuqi@nims.go.jp

1359-6462/$ - see front matter © 2011 Acta Materialia Inc. Published by Elsevier Ltd. All rights reserved.
doi:10.1016/j.scriptamat.2011.09.007

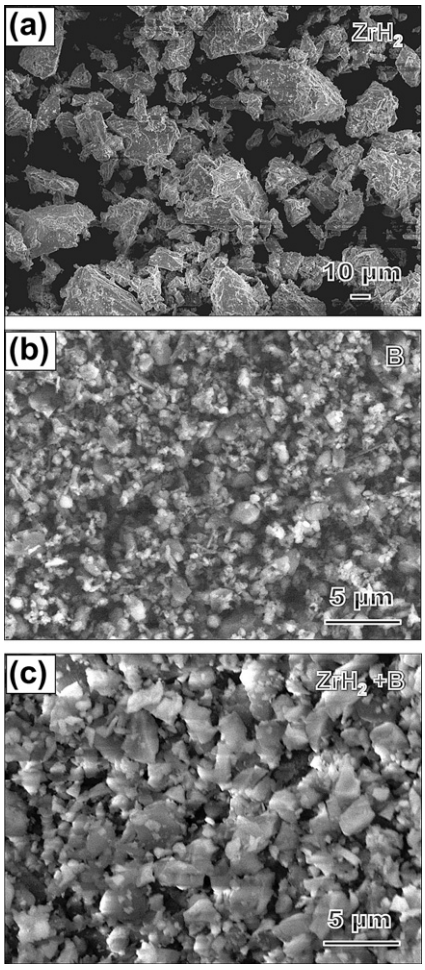

Figure 1. SEM images of (a) as-received ZrH_2, (b) amorphous B powders and (c) the milled ZrH_2–B powder mixture.

the particle size of the ZrH_2 powder significantly reduced with average size of ~2.5 μm. Fine B particles surrounded the large ZrH_2 particles.

A Dr. Sinter SPS-1030 apparatus (Simitomo Coal Mining Co. Ltd., Tokyo, Japan) was used in this study. The ZrH_2–B powder mixture was loaded into a graphite die lined with graphite foil. The in situ reactive sintering was conducted at temperatures of 1650–1800 °C with a heating rate of 100 °C min^{-1}, with a soaking time of 10 min in vacuum, under a uniaxial pressure of 50 MPa. The temperature of the sample was initially raised up to 600 °C within 2 min, and was then monitored by an optical pyrometer through a hole opened in the die and automatically regulated to the final sintering temperature. The pressure was applied at room temperature and held constant until the end of the sintering cycle. After sintering, the electric power was shut off to allow the sample to rapidly cool to room temperature (about 2 min for cooling from the sintering temperatures to 600 °C). The load was removed when the die temperature dropped to below 1000 °C. During the entire sintering process, the changes in the height of the samples with temperature along the pressing direction were recorded to monitor the densification behavior.

The final densities, ρ, of the sintered samples were measured by the Archimedes method with distilled water as medium. X-ray diffraction (XRD) was used to identify the crystalline phase presented in the prepared ZrB_2. The microstructure of the ZrB_2 was characterized by field emission scanning electron microscopy (FE-SEM). The grain size, d, was determined by measuring the average linear intercept length, d_m, of the grains in FE-SEM images of sintered ZrB_2 ceramics, according to the relationship $d = 1.56d_m$ [18].The thermal conductivity of the ZrB2, km, is determined from the thermal diffusivity, α, heat capacity, Cp, and density, ρ, according to the following equation [19]:

$$k_m = \rho C_p \alpha. \quad (2)$$

The thermal diffusivity was measured on a disk-shaped specimen with a diameter of 10 mm and thickness of 2 mm using the nanoflash technique (LFA447/2-4 N, NETZSCH-Geratebau GmbH, Germany). The heat capacity was determined with alumina as the reference material. In addition, the electrical conductivity of the ZrB_2 was measured using a four-wire probe at room temperature, by means of a power supply (Model: 6220, Keithley) and a digital multimeter (Model: 2182, Keithley) [20].

The shear modulus, G, Young's modulus, E, and Poisson's ratio, v, of the ZrB_2 were calculated using the longitudinal and transverse soundwave velocities which were measured in the ZrB_2 specimens by using an ultrasonic device [21]. Room-temperature four-point flexural strength was measured on bars with dimensions of 25 mm × 2.5 mm × 2 mm (inner span 10 mm, outer span 20 mm), with a crosshead speed of 0.5 mm min^{-1}. At least five specimens were used for each measurement.

In Figure 2, typical shrinkage curves obtained for the ZrH_2–B mixture during SPS cycles are presented. The shrinkage behavior observed was similar over the temperature range 1650–1800 °C. Typically, the shrinkage curves are divided into three different stages: I, II, and III. During stage I (600–850 °C), linear shrinkage behavior was observed with increasing temperature. A thermogravimetric study of the ZrH_2–B mixture showed that the reaction of ZrH_2 with B to form ZrB_2 occurred at ~500 °C and was accompanied by the decomposition of ZrH_2 [22]. At 900 °C or above, the ZrH_2–B mixture converted completely into ZrB_2 without trace quantities of residual ZrH_2 and B [22]. Thus, the occurrence of shrinkage was presumed to be a result of the volume contraction under pressure accompanied by the conversion of the ZrH_2–B mixture into ZrB_2 as well as with

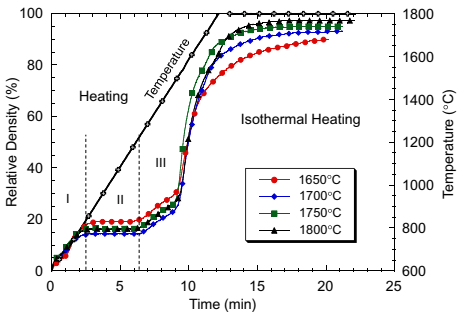

Figure 2. Typical shrinkage curves obtained during the SPS cycle at 1650–1800 °C for the milled ZrH_2–B powder mixture.

Table 1. Densities, relative densities, open porosity, closed porosity, and grain size of the ZrB_2 ceramics prepared by reactive SPS at 1650–1800 °C.

Materials	Processing conditions	Heating rate (°C/min)	Theoretical density (g/cm^3)	Measured density (g/cm^3)	Relative density (%TD)	Open porosity (%)	Closed porosity (%)	Grain size d (μm)	Lattice parameters (Å)	
									a	c
RS1	1650 °C/50 MPa/10 min	100	6.09	5.47	89.9	3.2	6.9	2.93 ± 1.14	3.169	3.531
RS2	1700 °C/50 MPa/10 min	100	6.09	5.69	93.4	0.2	6.4	3.99 ± 1.41	3.167	3.528
RS3	1750 °C/50 MPa/10 min	100	6.09	5.79	95.0	0.1	4.9	4.11 ± 1.63	3.167	3.531
RS4	1800 °C/50 MPa/10 min	100	6.09	5.92	97.2	0.1	2.7	5.35 ± 2.78	3.169	3.531

decomposition of ZrH_2. During stage II (850–1200 °C), the relative density remained almost constant with temperature. This means that the shrinkage of the reactive ZrB_2 powder did not initiate during this stage. This suggests that the densifying mechanism, such as grain boundary diffusion and grain boundary migration, was not activated during stage II. Stage III (>1200 °C) comprises two different regions, including a slow shrinkage region (1200–1500 °C) and a rapid shrinkage region (>1500 °C). This indicated that the densifying mechanism of the reactive ZrB_2 powder was activated above 1200 °C. At 1650 and 1700 °C, the densification was not completed during heating and carried on during subsequent isothermal heating for 10 min. At 1750 and 1800 °C, the majority of the densification occurred during heating. In particular, at 1800 °C noticeable shrinkage was observed only within a period of ~2 min following isothermal heating, and then a plateau was observed in the curve (Fig. 2). The measured densities of the ZrB_2 ceramics prepared by in situ reactive SPS are summarized in Table 1. Theoretical densities of 90% and 93% were obtained for the ZrB_2 ceramics prepared at 1650 and 1700 °C, respectively. Densities exceeding 95% were obtained at 1750 °C or above.

Compared with conventional ZrB_2 powder, SPS of which typically required 1900 °C to yield highly dense compacts [23], the in situ reactive ZrB_2 powder had a lower onset temperature of densification as well as a lower onset temperature of rapid densification, and therefore densification occurred at lower temperatures (Fig. 2). This suggests that the driving force for densification was significantly higher in the reactive ZrB_2 powder than in conventional ZrB_2 powder. It is known that densification of conventional ZrB_2 powder generally requires very high temperatures [4,23], owing to the covalent character of the bonding as well as to the low volume and grain boundary diffusion rates [2,3]. Unlike conventional ZrB_2 powder, the ZrB_2 produced by reactive SPS is presumed to form via the diffusion of B atoms into ZrH_2, forming ZrB_2 in situ and releasing H_2 gas. This reaction process occurred in stage I where the ZrH_2–B mixture converted into ZrB_2, with a fine grain size due to the very fine starting B powder [22]. Additionally, an early study of ZrB_2 ceramics produced by in situ reaction processes showed high defect concentrations in the materials [24]. Furthermore, the high defect concentrations are thought to promote densification [25]. Recently, Chamberlain et al. [26] showed that highly dense ZrB_2 ceramic was obtained at 1800 °C by reactive hot pressing an attrition-milled mixture of Zr and B powders. They concluded that the in situ reaction/densification process may enable low-temperature densification due to a combination of fine particles and high defect concentrations. Similar causes are expected for the ZrB_2 ceramics investigated in this study.

In Figure 3, XRD patterns of the resulting ZrB_2 ceramics are presented. The ZrB_2 is a primary crystalline phase and a trace amount of ZrO_2 is also present, while ZrH_2 is absent. The trace quantities of ZrO_2 may be attributed to oxygen uptake during the milling and/or handling procedures. The lattice parameters of the ZrB_2 samples were determined (Table 1) and their values are nearly identical to those of pure hexagonal ZrB_2 phase (a = 3.168 Å, c = 3.530 Å, PDF #34-0423). The microstructure of the ZrB_2 ceramics is observed under backscattered electron FE-SEM imaging, typical examples of which are shown

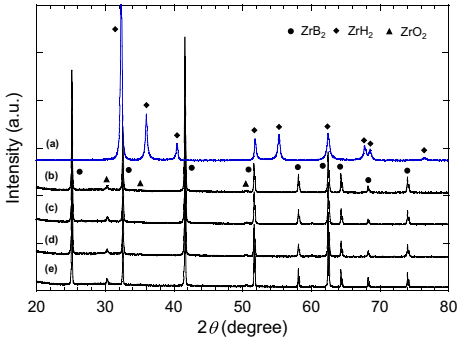

Figure 3. XRD patterns of the ZrB_2 ceramics prepared by reactive SPS at 1650–1800 °C: (a) before sintering; (b) 1650 °C; (c) 1700 °C; (d) 1750 °C; (e) 1800 °C.

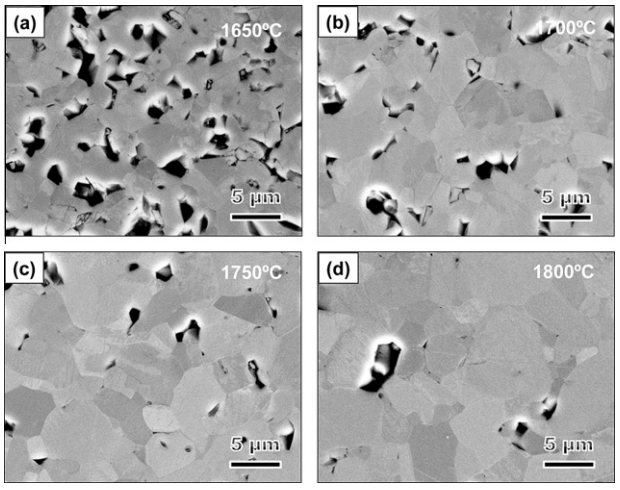

Figure 4. Typical examples of backscattered electron FE-SEM images of the ZrB_2 ceramics prepared by reactive SPS at 1650–1800 °C.

Table 2. Electrical conductivity, thermal and elastic properties, and flexural strength measured at room temperature for the ZrB_2 ceramics prepared by the reactive SPS at 1650–1800 °C.

Materials	Electrical conductivity σ (Ω^{-1} cm^{-1})	Thermal properties			Elastic properties			Flexural strength
		Cp (J g^{-1} K^{-1})	α (mm^2/s)	k_m (W(m K)$^{-1}$)	G (GPa)	E (GPa)	v	σ_{FS} (MPa)
RS1	6.44×10^4	0.52 ± 0.01	41.55 ± 0.49	119.22 ± 1.42	196	441	0.12	333 ± 61
RS2	5.98×10^4	0.50 ± 0.01	43.40 ± 0.19	124.22 ± 0.53	197	445	0.13	351 ± 30
RS3	6.18×10^4	0.50 ± 0.01	44.12 ± 0.12	127.36 ± 0.35	217	487	0.13	435 ± 44
RS4	7.01×10^4	0.51 ± 0.01	43.72 ± 0.14	133.01 ± 0.43	213	498	0.17	491 ± 22

in Figure 4. The ZrB_2 ceramics showed homogeneous microstructures that consisted of the equiaxed ZrB_2 grains. Although the ZrO_2 phase was detected by XRD (Fig. 3), FE-SEM observation failed to identify this phase. It should be presumed to be present in the grain boundaries. The ZrB_2 grains were coarsened with an increase of sintering temperature, and had an average size range of 2.93–5.35 μm (Table 1). In addition, many pores were observed for the samples prepared at 1650 °C. Larger pores were present at multi-grain pockets, whereas small pores were present at two-grain boundaries and/or were entrapped within the grains. An open porosity of 3.2% and a closed porosity of 6.9% were observed for the sample prepared at 1650 °C (Table 1). An increase in temperature caused a rapid decrease in the open porosity. At 1700 °C, most pores were found to be closed, and any further increase in temperature decreased the level of closed porosity. At 1750 °C or above, only a few closed pores were observed.

The electrical conductivity, thermal and elastic properties, and flexural strength of the prepared ZrB_2 ceramics are summarized in Table 2. The Young's modulus of the ZrB_2 ceramics increased from 441 to 498 GPa with increasing sintering temperature as a result of the decrease of porosity (Table 1) [21]. The flexural strength was in the range 333–491 MPa. The increase in sintering temperature led to an increase of the flexural strength and a narrow strength distribution, as a result of the decrease in the number of larger flaws in the resulting ZrB_2 that accompanied the densification. Moreover, the ZrB_2 ceramics have high thermal and electrical conductivities, which are dependent on sintering temperature. The thermal conductivities significantly increase with an increase of sintering temperature, as a result of porosity decrease and grain coarsening (Table 1) [11]. The electrical conductivities observed for the ZrB_2 ceramics were in the range of conductor materials, indicating that this material is a good electrical conductor. These properties are comparable with those of ZrB_2 ceramics produced by consolidating conventional ZrB_2 powder by hot-pressing and/or SPS [13].

In summary, monolithic ZrB_2 ceramics were successfully prepared by in situ reactive SPS of ZrH_2 and B powders at 1650–1800 °C. Highly dense ZrB_2 ceramics could be consolidated by reactive SPS at a lower temperature than that employed when using ZrB_2 powder. The relative densities of the resulting ZrB_2 ceramics increased with an increase in sintering temperature. Relative densities exceeding 95% were obtained at 1750 °C or above for the ZrH_2–B mixture. The resulting ZrB_2 ceramics consisted of homogeneous equiaxed grains which coarsened with increasing sintering temperature, with the average size range 2.93–5.35 μm. The Young's moduli increased with sintering temperature from 441 to 498 GPa. The flexural strength was in the range 333–491 MPa. The thermal conductivities were in the range 119.22–133.01 W m^{-1} K^{-1}, depending on the grain size and number of pores. The electrical conductivities were in the range 5.98×10^4–7.01×10^4 Ω^{-1} cm^{-1}.

[1] K. Upadhya, J.-M. Yang, W.P. Hoffmann, Am. Ceram. Soc. Bull. 76 (1997) 51.
[2] M. Pastor, Metallic borides: preparation of solid bodies. sintering methods and properties of solid bodies, in: V.I. Matkovich (Ed.), Boron and Refractory Borides, Springer Verlag, New York, 1977, pp. 457–493.
[3] G.A. Meeson, A.F. Gorbunow, Inorg. Mater. 4 (1968) 267.
[4] S.Q. Guo, J.-M. Yang, H. Tanaka, Y. Kagawa, Comp. Sci. Technol. 68 (2008) 3033.
[5] F. Monteverde, A. Bellosi, Scripta Mater. 46 (2002) 223.
[6] F. Monteverde, A. Bellosi, Adv. Eng. Mater. 5 (2003) 508.
[7] F. Monteverde, A. Bellosi, Solid State Sci. 7 (2005) 622.
[8] W.C. Trip, H.H. Davis, H.C. Graham, Am. Ceram. Soc. Bull. 52 (1973) 612.
[9] S.C. Zhang, G.E. Hilmas, W.G. Fahrenholtz, J. Am. Ceram. Soc. 89 (2006) 1544.
[10] D. Sciti, F. Monteverde, S. Guicciardi, G. Pezzotti, A. Bellosi, Mater. Sci. Eng. A A434 (2006) 303.
[11] S.Q. Guo, Y. Kagawa, T. Nishimura, H. Tanaka, Scripta Mater. 58 (2008) 579.
[12] F. Monteverde, A. Bellosi, S. Guicciardi, J. Eur. Ceram. Soc. 22 (2002) 279.
[13] S.Q. Guo, J. Euro. Ceram. Soc. 29 (2009) 995.
[14] P. Hu, Z. Wang, J. Euro. Ceram. Soc. 30 (2010) 1021.
[15] G.J. Zhang, Z.Y. Deng, N. Kondo, J.F. Yang, T. Ohji, J. Am. Ceram. Soc. 83 (2000) 2330.
[16] W.W. Wu, G.J. Zhang, Y.M. Kan, P.L. Wang, J. Am. Ceram. Soc. 89 (2006) 2967.
[17] M. Brochu, B. Gauntt, T. Zimmerly, A. Ayala, R. Loehman, J. Am. Ceram. Soc. 91 (2008) 2815.
[18] M.I. Mendelson, J. Am. Ceram. Soc. 52 (1969) 443.
[19] W.J. Parker, W.J. Jenkins, C.P. Butler, G.L. Abbott, J. Appl. Phys. 32 (1961) 1679.
[20] S.Q. Guo, R. Sivakumar, H. Kitazawa, Y. Kagawa, J. Am. Ceram. Soc. 90 (2007) 1667.
[21] S.Q. Guo, Y. Kagawa, T. Nishimura, H. Tanaka, Ceram. Int. 34 (2008) 1811.
[22] S.Q. Guo, C. Hu, Y. Kagawa, J. Am. Ceram. Soc., in press, doi:10.1111/j.1551-2916.2011.04825.x.
[23] S.Q. Guo, T. Nishimura, Y. Kagawa, J.-M. Yang, J. Am. Ceram. Soc. 91 (2008) 2848.
[24] S.K. Mishra, S. Das, L.C. Pathak, Mater. Sci. Eng. A A364 (2004) 249.
[25] P.S. Kisliy, M.A. Kuzenkova, O.V. Zaveruha, Phys. Sintering 4 (1972) 107.
[26] A.L. Chamberlain, W.G. Fahrenboltz, G.E. Hilmas, J. Am. Ceram. Soc. 89 (2006) 3638.